JOURNAL OF LEUKOCYTE BIOLOGY

Check for updates

ARTICLE

Paeoniflorin relieves LPS-induced inflammatory pain in mice by inhibiting NLRP3 inflammasome activation via transient receptor potential vanilloid 1

Nina Yin[1] | **Qinghua Gao[2]** | **Wenting Tao[2]** | **Jiaojiao Chen[2]** | **Jing Bi[3]** | **Fengmin Ding[2]** | **Zhigang Wang[3]** iD

[1]Department of Anatomy, School of Basic Medical Sciences, Hubei University of Chinese Medicine, Wuhan, China

[2]School of Basic Medical Sciences, Hubei University of Chinese Medicine, Wuhan, China

[3]Department of Pathogen Biology, School of Basic Medical Sciences, Hubei University of Chinese Medicine, Wuhan, China

Correspondence
Fengmin Ding, School of Basic Medical Sciences, Hubei University of Chinese Medicine, 16 Huangjiahu West Road, Hongshan District, Wuhan 430065, China.
Email: dingfm@126.com
Dr. Zhigang Wang, Department of Pathogen Biology, School of Basic Medical Sciences, Hubei University of Chinese Medicine, 16 Huangjiahu West Road, Hongshan District, Wuhan 430065, China.
Email: wangzg@hbtcm.edu.cn

Abstract

LPS has been widely used to induce inflammatory pain, attributing to production of inflammatory cytokines and sensitization of nociceptors. Paeoniflorin (PF) possesses anti-nociceptive property, but its effect on LPS-induced inflammatory pain has not been investigated. In this study, we aimed to investigate the analgesic effect of PF on an inflammatory pain mouse model and explore the underlying mechanisms. LPS-induced inflammatory pain model was established in C57BL/6J mice after PF treatment. Then, thermal hyperalgesia, neutrophil infiltration, inflammatory cytokine production, intracellular Ca^{2+} levels, PKC activity, transient receptor potential vanilloid 1 (TRPV-1) expression, NF-κB transcription, and NLPR3 inflammasome activation were assessed by thermal withdrawal latency, histopathology, ELISA, intracellular Ca^{2+} concentration, immunohistochemistry, and Western blot, separately. PF significantly relieved inflammatory pain and paw edema in mice with LPS-induced inflammatory pain. Additionally, PF inhibited neutrophil infiltration, inflammatory cytokine production (IL-1β, TNF-α, and IL-6), intracellular Ca^{2+} levels, and PKC activity as well as suppressed TRPV-1 expression, NF-κB transcription, and NLPR3 inflammasome activation in the footpad tissue samples. Importantly, capsaicin (TRPV-1 agonists) obviously reversed the pain-relieving effect of PF, suggesting the involvement of TRPV-1 in the analgesic activity of PF. Our results indicated PF ameliorated LPS-induced inflammation and pain in mice by inhibiting TRPV-1-mediated NLRP3 inflammasome activation. These findings suggest that PF can be as a potential pharmacological agent for inflammatory pain and thus deserves more attention and further investigation.

KEYWORDS
Ca2+/PKC cascade, capsaicin, hyperalgesia, inflammation

1 | INTRODUCTION

Pain is an unpleasant sensory and emotional experience often caused by intense or damaging stimuli. Woolf suggests three classes of pain: nociceptive pain, pathological pain, and inflammatory pain.[1] Inflammatory pain results from the sensitization and activation of peripheral nociceptors by pro-inflammatory mediators, such as IL-1β, TNF-α, bradykinin, prostaglandins, and serotonin (5-HT), which accumulate at the site of inflammation thereby leading to become inflamed and often red, swollen, and hot.[2] Furthermore, the amplification of inflammatory mediators upon primary sensory afferents leads to a lowered threshold for activation and increased responsiveness, resulting in hyperalgesia, allodynia, and spontaneous pain.[3]

Nucleotide-binding oligomerization domain (NOD)-like receptor (NLR) pyrin domain containing 3 (NLRP3) inflammasomes, consisting of NLRP3, apoptosis-associated speck-like protein containing (ASC), and caspase-1, are assembled once receiving an activation signal.

NLRP3 forms a scaffold with ASC to activate pro-caspase-1, which subsequently promotes the cleavage of pro-IL-1β and pro-IL-18 into active IL-1β and IL-18 to release.[4] The inflammasome activation promotes the maturation of IL-1β and sensitizes the nociceptive neurons in the process of inflammatory hyperalgesia.[5] By contrast, inhibition of NLRP3/ASC/pro-caspase-1 inflammasome formation and activity prevented inflammatory hyperalgesia induced by LPS in mice.[6] A recent study showed that electroacupuncture (EA) relieved the inflammatory pain by inhibiting the activation of NLRP3 inflammasome.[7] Although some studies have reported the involvement of NLRP3 inflammasome activation in inflammatory pain, the underlying mechanisms are still worth of being deeply investigated, owing to the different experimental design and treatment.

Transient receptor potential vanilloid 1 (TRPV-1), a ligand–gated non-selective cation channel in the TRP family, is highly expressed in primary sensory neurons and acts as the endogenous transducer of noxious stimuli that cause pain, inflammation, and hyperalgesia.[8] Increasing evidence indicates that TRPV-1 plays a crucial role in the development of inflammatory pain. Mice lacking TRPV-1 failed to develop thermal hyperalgesia after complete Freund's adjuvant (CFA) or carrageenan administration.[9] TRPV-1 knockout mice had limited-edema and thermal hyperalgesia, and showed insignificant histological changes in models of inflammatory pain.[10] Due to its modulatory effect on inflammatory pain, TRPV-1 provides a possibility for therapeutic interventions in pain management.

Paeoniflorin (PF) is a major bioactive component of "Paeony root" with anti-inflammation, anti-allergy, and anti-nociceptive properties.[11] Accumulating data indicates the analgesic effect of PF on formalin-induced nociceptive behavior in mice,[12] neonatal maternal separation-induced visceral hyperalgesia in rats,[13] and CFA-induced inflammatory pain in mice.[14] A previous publication reported that PF inhibited TRPV-1-activated IL-8 and PGE$_2$ production in HaCaT cells,[15] suggesting a potential relationship between anti-inflammatory activity of PF and TRPV-1 signaling. However, little is known for the effect of PF on NLPR3 inflammasome activation further with inflammatory pain.

Herein, we hypothesize that PF might alleviate LPS-induced inflammatory pain by inhibiting NLRP3 inflammasome activation via TRPV-1 receptors. Our results indicated that the involvement of inhibiting TRPV-1-mediated NLRP3 inflammasome activation in the analgesic effect of PF on inflammatory pain.

2 | MATERIALS AND METHODS

2.1 | Animals

Male C57/BL6 mice (6 weeks old, 18–20 g) were obtained from the Hubei Research Center of Laboratory Animals (Wuhan, China) (No.: 42000600032539) and acclimated for 1 week before experiment. Mice were housed in a specific pathogen-free environment (22 ± 2°C and 60 ± 5% relative humidity) under 12/12 h light/dark cycle with free access to food and water at the Animal Care Facility of Hubei University of Chinese Medicine (Wuhan, China). Animal care and use were approved by the Animal Care and Use Committee of Hubei University of Chinese Medicine (No.: SYXK2017-0067) and also followed with the Guide for the Care and Use of Laboratory Animals published by the United States National Institutes of Health.

2.2 | Experimental protocol

2.2.1 | Experiment 1

Mice were randomly divided into 6 groups ($n = 8$ for each group): V (vehicle of PF injection), LPS (LPS injection), LPS + 1 mg/kg PF (LPS injection following low dose of PF treatment), LPS + 5 mg/kg PF (LPS injection following middle dose of PF treatment), LPS + 25 mg/kg PF (LPS injection following high dose of PF treatment), and PF (25 mg/kg) (vehicle of LPS injection following high dose of PF treatment).

As shown in Fig. 1A, mice were i.p. injected daily with PF ($\geq$98% purity by HPLC analysis, P0038, Sigma–Aldrich, St. Louis, MO, USA) or the same volume of sterilized saline (vehicle of PF) continuously for 1 week, separately. Two hours after last injection on the seventh day, LPS (200 ng/20 μL) (*Escherichia coli* 0111: B4) (L2630, Sigma–Aldrich) or the same volume of sterilized saline (vehicle of LPS) was injected into the plantar surface of right hind paw using a microsyringe with a 30-gauge needle, respectively.[16] After 5 h, mice were sacrificed by cervical dislocation and samples were collected for further evaluation.

According to the results of Fig. 1, four groups were observed in subsequent experiments: V (vehicle of PF injection), LPS (LPS injection), LPS + PF (LPS injection following 25 mg/kg PF treatment), and PF (vehicle of LPS injection following 25 mg/kg PF treatment).
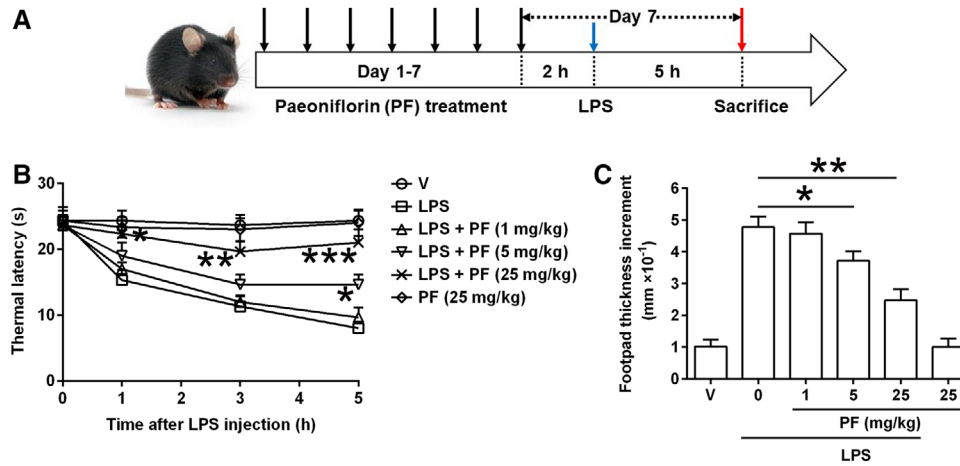
2.2.2 | Experiment 2

Mice were randomly divided into four groups ($n = 8$ for each group): LPS (LPS injection), LPS + PF (LPS injection following 25 mg/kg PF treatment), Capsaicin + LPS + PF, and Capsaicin (capsaicin application).

As shown in Fig. 6A, PF (25 mg/kg) was i.p. injected into mice continuously for 7 days as described above. Simultaneously, mice were subjected to capsaicin (TRPV-1 agonists, 0.05 mg/kg; S1990, Selleckchem, Houston, TX, USA) via s.c. injection, and the total dose was administrated equally by 3 times (Day 1–3).[17,18] Two hours after last injection on the seventh day, LPS (200 ng/20 μL) was applied under the plantar surface of right hind paw. Mice were sacrificed 5 h after LPS challenge by cervical dislocation and samples were collected for further evaluation.

2.3 | Thermal withdrawal latency test

Thermal nociceptive threshold was assayed through measuring withdrawal latency on hot plate as previous described. The temperature of the hot-plate was maintained at 50°C. The withdrawal latency started from putting the mouse on the plate and terminated when a brisk withdrawal or paw flinching was observed with a cutoff of 30 s. The test was repeated 3 times in each mouse and the mean value was calculated for evaluation.

FIGURE 1 Effects of PF on LPS-induced thermal hyperalgesia and paw edema in mice with inflammatory pain. (A) Schematic diagram of experiment 1 as described in experimental protocols. Briefly, Vehicle (V, saline) or PF was i.p. injected into mice continuously for 7 days ($n = 8$ per group). 2 h after last injection, LPS (200 ng/20 μL) was used via i.p. injection. After 5 h, mice were sacrificed by cervical dislocation and samples were collected. (B) Thermal hyperalgesia was evaluated by time course of the paw withdrawal latency at the indicated time points after LPS injection using a hot plate apparatus. (C) Paw edema was measured and analyzed by the footpad thickness increment. *$P < 0.05$, **$P < 0.01$, and ***$P < 0.001$

2.4 | Footpad swelling assay

Footpad thicknesses were measured in a blinded fashion using a thickness gauge (Digimatic caliper, Mitutoyo, Japan) at 24 h after LPS challenge. The magnitude of LPS-induced footpad swelling was determined as follows: Footpad thickness increment = thickness of LPS-challenged footpad (right) − thickness of unchallenged footpad (left).

2.5 | Histopathological assessment

Mice were sacrificed at the end of experiment, and the right hind footpad was removed and fixed in 4% paraformaldehyde. After paraffin embedding, tissue sections (5 μm) (Cryostat CM3050S, Leica Microsystems, Germany) were stained with hematoxylin and eosin (H&E) to observe inflammatory cell infiltration, and images were taken using Olympus BX60 (Olympus Optical Co Ltd, Japan). All sections were randomized and evaluated by two independent investigators in a blinded manner.

2.6 | Cytokine detection by ELISA

Footpad tissue samples of different groups were collected, weighed, and homogenized in 1 ml of tissue protein extraction reagent containing a protease inhibitor cocktail (Pierce, Rockford, IL, USA). Homogenates were centrifuged at 12,000 $\times$ g for 15 min at 4°C to obtain the supernatant. Cytokine productions, including IL-1β (BGK10749), TNF-α (BGK06804), and IL-6 (BGK08505), were determined by ELISA (PeproTech, Rocky Hill, NJ, USA) according to the manufacturer's instructions using an iMark™ Microplate Absorbance Reader (Bio-Rad Laboratories, Inc., Richmond, CA, USA). All experiments were done in triplicate.

2.7 | Immunohistochemical analysis

The tissue sections were deparaffinized and rehydrated following a standard procedure. The endogenous peroxidase activity was then quenched with 3% H_2O_2 in methanol and blocked with normal goat serum. Anti-mouse TRPV-1 polyclonal antibody (PA1-29421, Invitrogen, Carlsbad, CA, USA) were applied onto each section overnight, respectively. Then, the slides were incubated with poly-HRP reagent. Staining was visualized by incubating with 3,3′-diaminobenzidine followed by hematoxylin counter staining. Under ×400 magnification, the morphometric examination was observed by 2 independent investigators in a blinded manner. For each section, five visual fields were chosen at random and the mean number of the positive cells were counted and represented.

2.8 | Immunofluorescence

After mice were sacrificed, the skin tissues of right hind footpad were quickly removed, fixed in 4% paraformaldehyde for 6 h, and cryoprotected in 30% sucrose for 48 h at 4°C. The sections were cut at 10 μm on a cryostat and mounted onto gelatin-coated slides followed by air-dried overnight. For immunofluorescence labeling, the slides were rinsed in 0.1 M PBS, blocked for 1 h with 2% BSA, and then incubated with the following primary antibodies at 4°C overnight: Rabbit anti-CD68 (14-0681-82) (Invitrogen) and Rat anti-NLRP3 (MA5-23919) (Invitrogen). For labeling, the primary Abs were detected with corresponding secondary Abs (Jackson ImmunoResearch, West Grove, PA, USA): donkey anti-rabbit IgG conjugated with Alexa Fluor®488 (711-545-152) or donkey anti-rat IgG conjugated with Alexa Fluor®594 (712-585-150). Lastly, the sections were stained with DAPI (AR1177) (Boster Biological Technology, Wuhan, China) and examined under a fluorescence microscope (Olympus BX50, Tokyo, Japan). A total of 5 sections were imaged from the same skin tissues per mouse, and 3 visual fields were chosen at random for each section. CD68^{+}NLRP3^{+}

positive cells were counted in non-overlapping areas of high-power field and represented as the percentage of 100 Mφs (CD68⁺) per slide.

2.9 | Detection of intracellular Ca^{2+} concentration

Footpad tissue samples were homogenized and centrifuged to obtain the supernatant as above described. Intracellular Ca^{2+} concentration was determined with a BioVision kit (K380-250, BioVision Inc., Mountain View, CA, USA) according to the manufacturer's protocol, and absorbance was measured at 575 nm using a micro-plate reader (Bio-Rad Laboratories).

2.10 | Measurement of PKC activity

Footpad tissues samples were homogenized and centrifuged to obtain the supernatant as above described. Levels of PKC activity were measured using a PKC activity assay kit (ADI-EKS-420A, Enzo Life Sciences, Inc., Farmingdale, NY, USA) according to the manufacturer's instructions. Absorbance was measured at 450 nm with a microplate reader (Bio-Rad Laboratories) and the enzyme activity was expressed as a relative activity.

2.11 | Western blotting

Footpad tissue samples were collected for protein extraction on ice using a Nuclear Protein and Cytosolic Protein Extraction Kit (P0028, Beyotime Institute of Biotechnology) according to the manufacturer's instructions. Protein samples (25 μg) were loaded and separated by 10% serum dodecyl sulfate-polyacrylamide gels (SDS-PAGE). Then, the gels were electro-transferred onto polyvinylidene difluoride (PVDF) membranes (Millipore, Billerica, MA, USA). After blocking with 5% non-fat dry milk for 2 h at room temperature, the membranes were incubated with the primary Abs against TRPV-1 (PA1-29421, Invitrogen), PKCε (ab63387), NF-κB (p-p65) (ab28856), NLPR3 (ab210491), cleaved Caspase-11 (p26) (ab180673), GAPDH (ab181602), Lamin B1 (ab16048; Abcam, Cambridge, MA, USA), ASC (#67824S), cleaved Caspase-1 (p20; #89332S), and cleaved IL-1β (p17) (#52718S; Cell Signaling Technology, Danvers, MA, USA) overnight at 4°C. Subsequently, the horseradish peroxidase-conjugated secondary Ab (ab6721, Abcam) were used to incubate the membranes for 2 h at room temperature. Peroxidase-labeled protein bands were detected and analyzed with ImageJ software (National Institutes of Health, Bethesda, MD, USA).

2.12 | Statistical analysis

Data were analyzed using GraphPad Prism 7.0 software (GraphPad Software, La Jolla, CA, USA) and results were presented as means ± SD. Difference between two groups were compared by an unpaired Student's t-test, and among multiple groups by one-way ANOVA followed by Tukey's post hoc test. Curve estimation and linear regression analyses were performed for correlation analysis. $P < 0.05$ indicated statistical significance.

3 | RESULTS

3.1 | PF relieves LPS-induced inflammatory pain and paw edema in mice

First, mice were treated with different concentrations of PF before LPS injection (Fig. 1A). Then, thermal hyperalgesia was assessed by time course of the paw withdrawal latency at the indicated time points. As shown in Fig. 1B, 5 mg/kg of PF obviously inhibited thermal hyperalgesia induced by LPS at 5 h. High-dose PF (25 mg/kg) significantly relieved LPS-induced hyperalgesia at 3 and 5 h, separately. Additionally, LPS injection induced paw edema compare to Vehicle group, while PF (5 and 25 mg/kg) clearly decreased the footpad thickness increment (Fig. 1C). Base on the initial data, the dose of 25 mg/kg was used in the following experiments.

3.2 | PF reduces LPS-induced neutrophil infiltration and inflammatory cytokine production
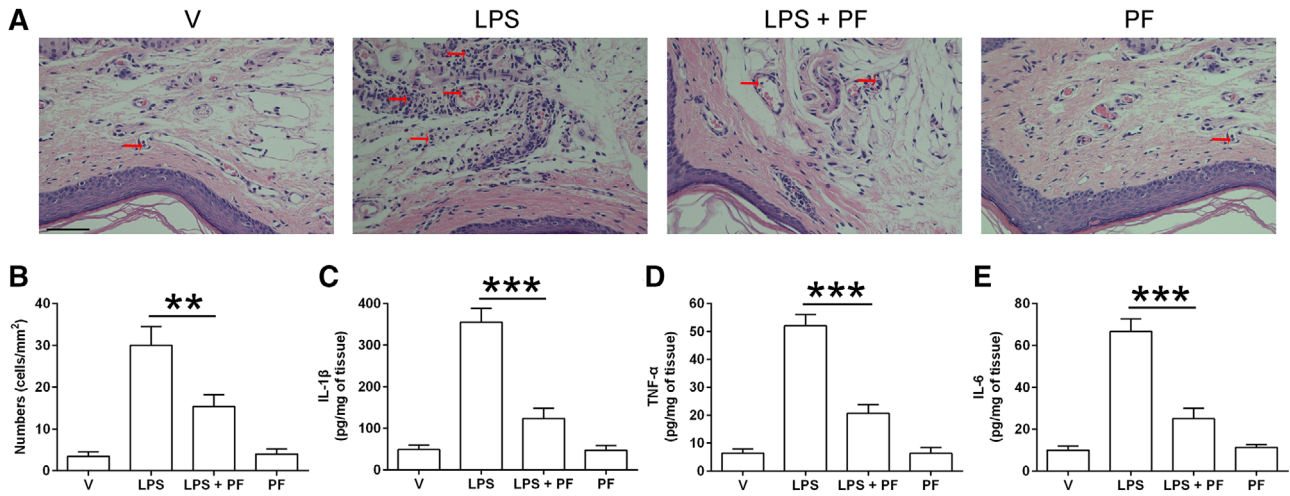
Neutrophil infiltration and inflammatory cytokine production are important indicators in the process of inflammatory pain. Therefore, we investigated histological change and inflammatory cytokine production in the footpad tissues. The results showed that the number of neutrophils in LPS + PF group was notably decreased compared with those in single LPS-injected group (Fig. 2A and B). Moreover, PF treatment significantly reduced LPS-induced inflammatory cytokine production, such as of IL-1β, TNF-α, and IL-6 (Fig. 2C–E). These data suggest that PF could relieve inflammatory pain, at least partly, by inhibiting the neutrophil recruitment and inflammatory cytokine release.

## 3.3 | PF suppresses NF-κB transcription and NLPR3 inflammasome activation

To explore the underlying mechanisms associated with the antinociceptive effect of PF, NF-κB transcription, and NLRP3 inflammasome activation were determined under PF treatment. As shown in Fig. 3A-C, Western blot data indicated that PF significantly suppressed the expression of cytosolic PKCε protein and nuclear NF-κB (p65) transcription. Moreover, PF evidently curbed the expression of cytosolic NLPR3, ASC, cleaved Caspase-11 (p26), cleaved Caspase-1 (p22), and cleaved IL-1β (p17) proteins in LPS-challenged mice (Fig. 3D–I).
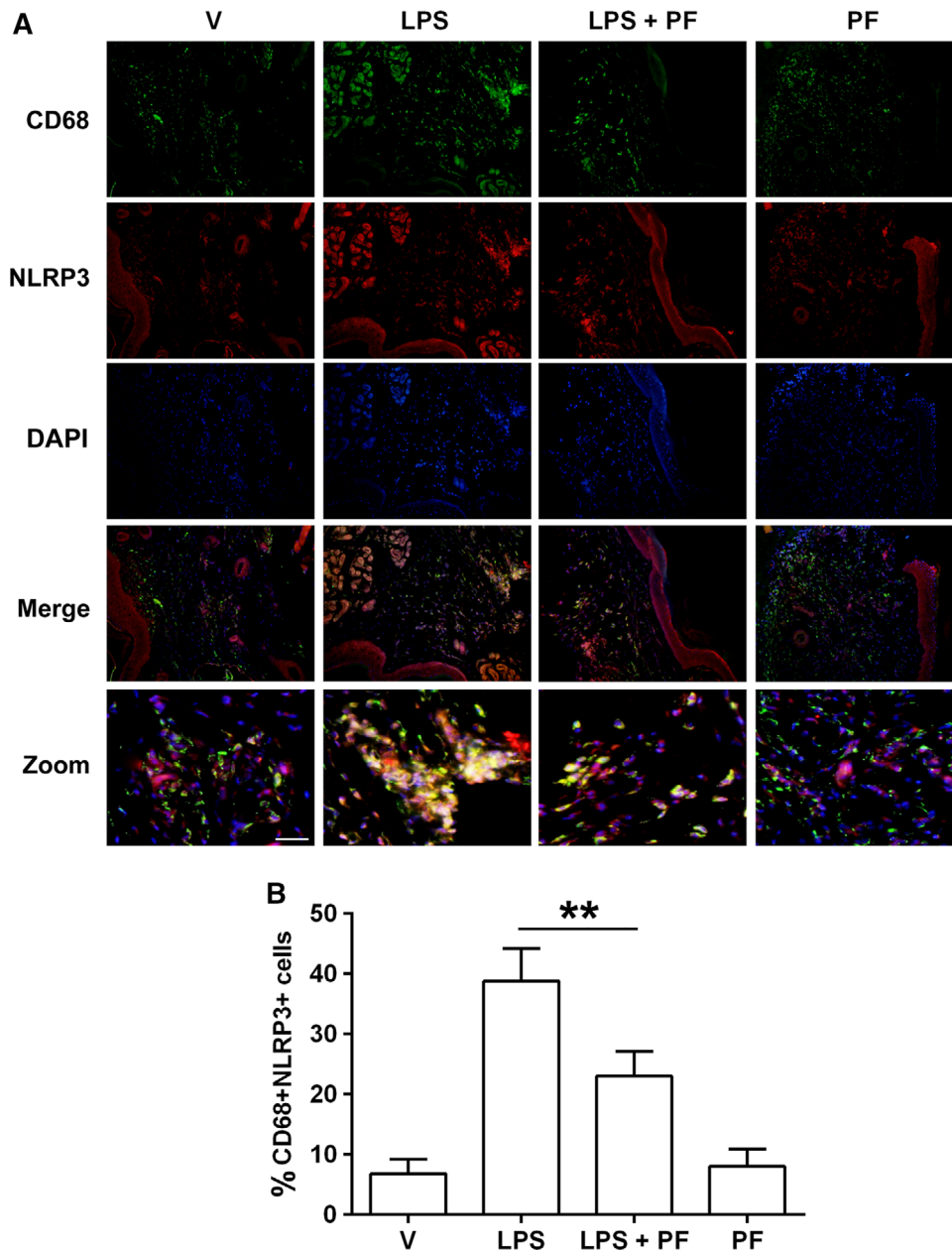
3.4 | PF curbs NLRP3 inflammasome activation in Mφs

Next, we investigated the expression of NLRP3 in Mφs located in inflamed skin tissues. Double immunofluorescence labeling showed that NLPR3 was colocalized with CD68, a marker for Mφs. Compared with the vehicle group, LPS significantly increased the number of cells double labeled with CD68 and NLRP3 in the skin tissue sections. PF application evidently decreased the percentage of CD68⁺NLRP3⁺ cells in CD68⁺ Mφs (Fig. 4A and B). These finding suggest that PF

FIGURE 2 **Effect of PF on LPS-induced inflammatory responses.** (**A**) Footpad tissues of different groups were obtained and stained with HE. Red arrow indicated neutrophil infiltration. Scar bar = 50 μm. (**B**) The number of neutrophils in footpad tissue sections of different groups were counted and statistically analyzed. (**C–E**) Levels of inflammatory cytokines in homogenized footpad tissues were assessed by ELISA, such as IL-1β, TNF-α, and IL-6. **$P < 0.01$ and ***$P < 0.001$
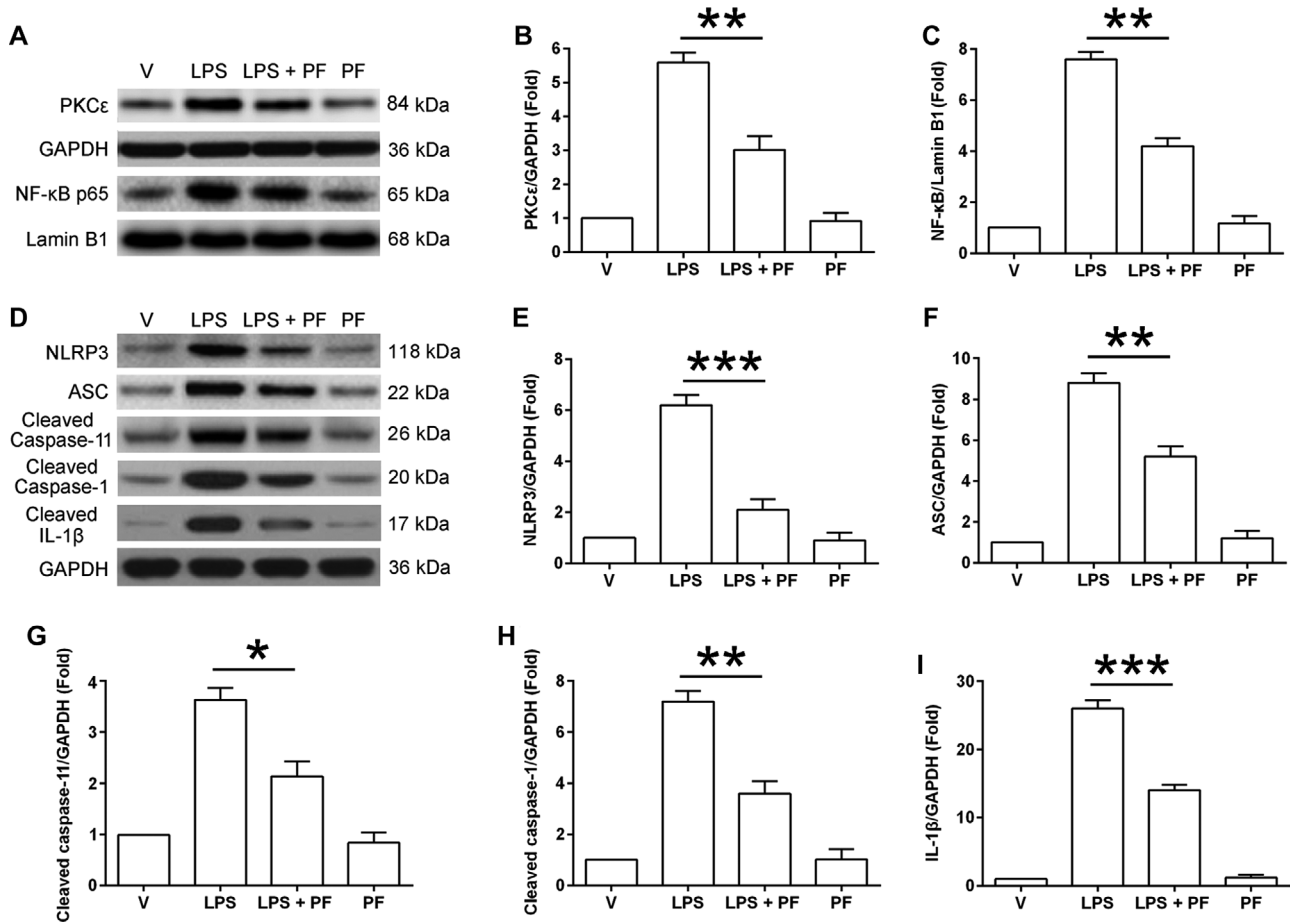
FIGURE 3 **Effects of PF on NF-κB transcription and NLPR3 inflammasome activation.** Footpad samples of different groups were collected and lysed. Then, cytosolic and nuclear proteins were extracted respectively for Western blot assay. (**A–C**) Representative Western blot showed the expression of cytosolic PKCε and nuclear NF-κB (p65) proteins. (**D–I**) Representative Western blot indicated the expression of cytosolic NLRP3, ASC, cleaved Caspase-11 (p26), cleaved Caspase-1 (p20), and cleaved IL-1β (p17) proteins. The relative protein level (fold) was shown and statistically analyzed. GAPDH and Lamin B1 were used to confirm equal sample loading, respectively. **$P < 0.01$ and ***$P < 0.001$

FIGURE 4 Effects of PF on NLRP3 inflammasome activation in Mϕs located in inflamed footpad tissues. (**A**) Immunofluorescence images of footpad skin sections showed CD68 positive-Mϕs (green) and NLRP3-immunoreactive cells (red). Cell nuclei were stained with DAPI (blue). Merge panels were overlay images presenting triple-labeled cells. Zoom panels were magnified images of the merge panels. Scar bar = 50 μm. (**B**) The percentage of CD68$^+$NLRP3$^+$ cells in tissue sections from the different groups were counted and statistically analyzed. **$P < 0.01$

treatment reduces the expression of NLRP3 in Ms recruited into inflamed skin tissues.

3.5 | PF decreases intracellular Ca^{2+} levels and PKC activity

In view of the relevance of Ca^{2+} mobilization and LPS-induced inflammatory pain, we further assessed the effects of PF on intracellular Ca^{2+} levels and the downstream PKC activation. Comparison with single LPS-injected group, PF treatment markedly decreased intracellular Ca^{2+} concentration and suppressed PKC activity (Fig. 5A and B).

Furthermore, correlation analysis showed that the ratio of intracellular Ca^{2+} concentration (LPS + PF group/LPS group) was positive correlation with the ratio of IL-1β concentration (LPS + PF group/LPS group) ($r = 0.9489$, $P = 0.0003$) and TNF-α ($r = 0.9541$, $P = 0.0002$), respectively (Fig. 5C and D).

3.6 | PF inhibits TRPV-1 expression in mice with inflammatory pain

Considering that TRPV-1 channels participate in NLPR3 inflammasome activation, we further investigated the effect of PF on
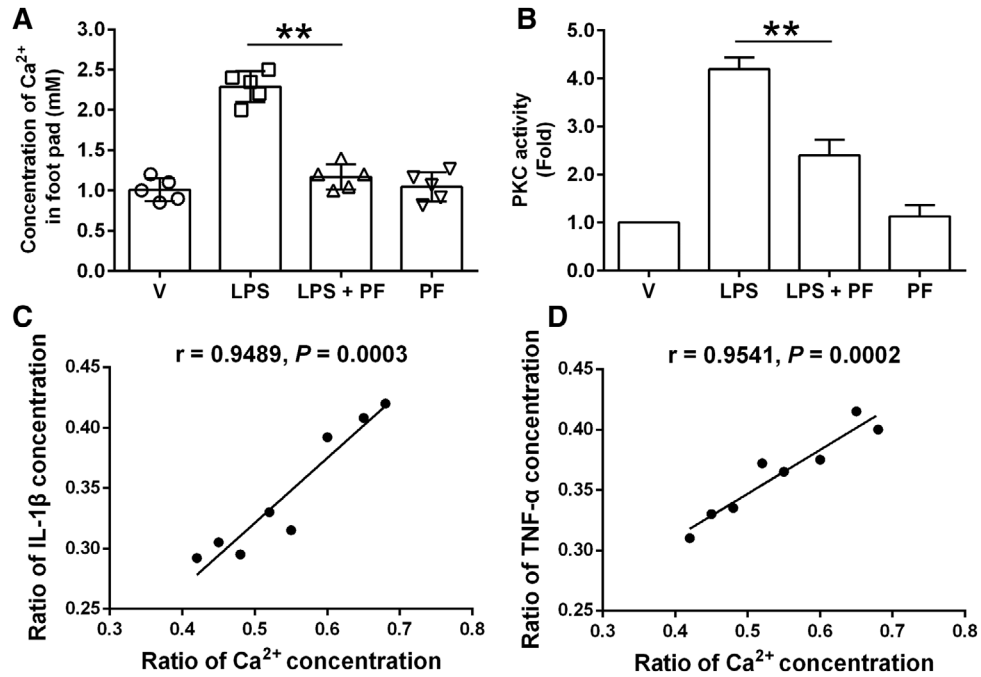
FIGURE 5 Effects of PF on intracellular Ca^{2+} concentration and PKC activity. At the end of the experiment 1, footpad tissues of different groups were collected and homogenized. (**A** and **B**) Intracellular Ca^{2+} concentration and the levels of PKC activity in different groups were measured and statistically analyzed. (**C**) Correlation analysis between the ratio of Ca^{2+} concentration (LPS + PF group/LPS group) and the ratio of IL-1β concentration (LPS + PF group/LPS group) ($r = 0.9489$ and $P = 0.0003$). (**D**) Correlation analysis between the ratio of Ca^{2+} concentration (LPS + PF group/LPS group) and the ratio of TNF-α concentration (LPS + PF group/LPS group) ($r = 0.9541$ and $P = 0.0002$). **$P < 0.01$
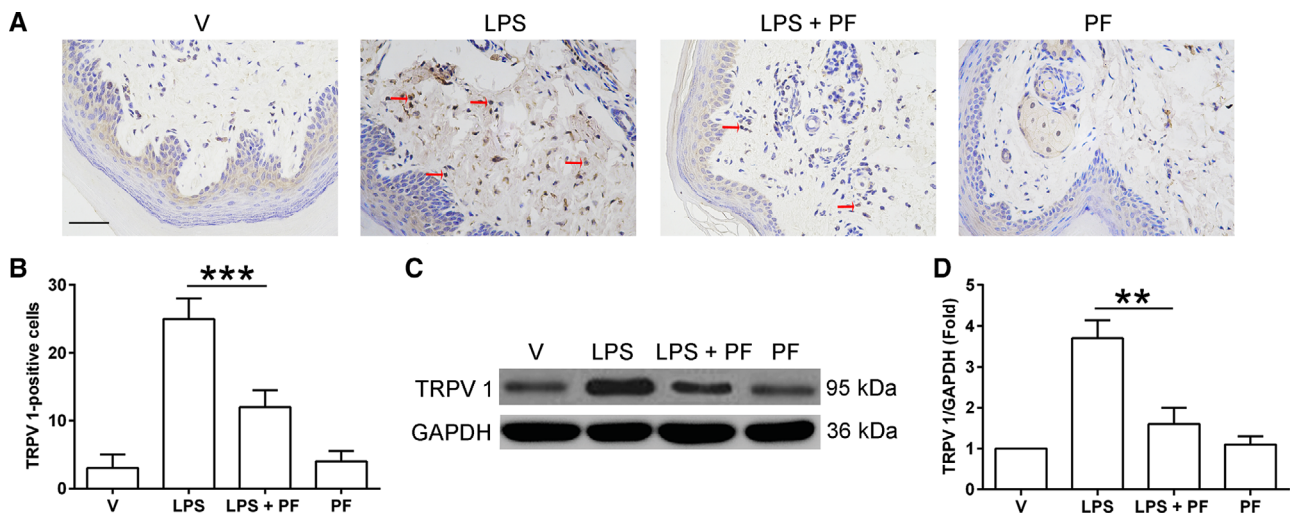

FIGURE 6 Effect of PF on TRPV-1 expression. (**A** and **B**) Representative immunohistochemical staining showed TRPV-1 expression in footpad tissues, and the statistical analysis of TRPV-1-positive cells in the different groups was shown. Red arrow indicated TRPV-1-positive cells. Scar bar = 50 μm. (**C** and **D**) The protein expression of TRPV-1 was assessed by Western blotting and statistical analysis was shown. A representative result was shown. **$P < 0.01$ and ***$P < 0.001$

TRPV-1 expression. Representative immunohistochemical staining showed TRPV-1 expression in footpad samples was visibly up-regulated after LPS administration. However, PF significantly decreased the number of TRPV-1-positive cells (Fig. 6A and B). Meanwhile, PF also greatly inhibited the expression of TRPV-1 protein in mice with LPS-induced inflammatory pain model (Fig. 6C and D).

3.7 | Involvement of TRPV-1 in the anti-nociceptive effect of PF

According to the schematic diagram of experiment 2, capsaicin (TRPV-1 agonists) was used to further evaluate the anti-nociceptive effect of PF on LPS-induced inflammatory pain (Fig. 7A). Capsaicin
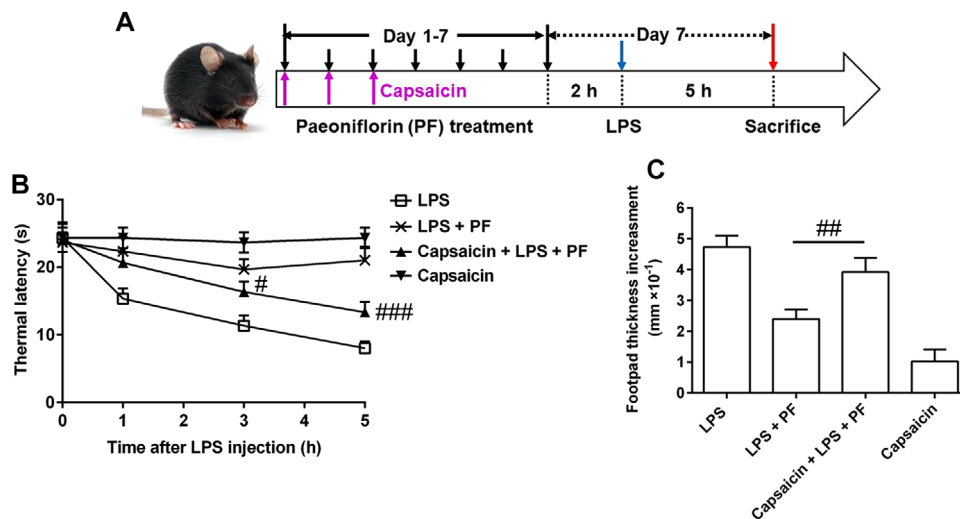
FIGURE 7 Effect of TRPV-1 agonists in mice with inflammatory pain. (A) Schematic diagram of the experiment II as described in experimental protocols. Briefly, Vehicle (V, saline) or PF was i.p. injected into mice continuously for 7 days ($n = 8$ per group). Simultaneously, capsaicin (TRPV-1 agonists, 0.05 mg/kg) was applied via s.c. injection, and the total dose was administrated equally by 3 times (Day 1–3). Two hours after last injection on the seventh day, mice were subjected to LPS (200 ng/20 μL) via i.pl. injection. (B) Thermal hyperalgesia was evaluated by time course of the paw withdrawal latency at the indicated time points after LPS injection using a hot plate apparatus. (C) Paw edema was measured and analyzed by the footpad thickness increment. $^{##}P < 0.01$ and $^{###}P < 0.001$

abrogated the inhibition of PF in LPS-induced thermal hyperalgesia and paw edema, although no obvious effect was presented in mice with single capsaicin treatment (Fig. 7B and C). As shown in Fig. 8A and B, capsaicin clearly enhanced TRPV-1 expression as specific agonists. Moreover, capsaicin reversed the suppressive activity of PF in inflammatory hyperalgesia, including inflammatory cytokine production (IL-1β and TNF-α), intracellular Ca^{2+} levels, and PKC activity (Fig. 8C-F).

3.8 | PF ameliorates LPS-induced inflammatory pain in mice associated with TRPV-1-mediated NLRP3 inflammasome activation

Lastly, NF-κB transcription and NLPR3 inflammasome activation were evaluated utilizing TRPV-1 agonists. Comparison with LPS + PF group, capsaicin application increased the expression of cytosolic PKCε protein. However, there was no obvious difference in nuclear NF-κB (p65) transcription with or without TRPV-1 agonists, which suggests that other signaling pathway might also participate in the analgesic effect of PF (Fig. 9A-C). Consistent with above results, capsaicin significantly reversed the reduction of cytosolic NLPR3, ASC, cleaved Caspase-11 (p26), cleaved Caspase-1 (p22), and cleaved IL-1β (p17) proteins under PF treatment (Fig. 9D-I).

4 | DISCUSSION

Inflammatory pain model is always established by intraplantar injection into the hind paw of murine with different biological substances, such as CFA, formalin, carrageenan, capsaicin, and LPS.[19-21] Generally, CFA injection induced a persistent inflammatory pain, formalin was

used to detect the spontaneous nociceptive pain behaviors to chemical stimulation, and capsaicin evoked spontaneous pain behavior and hypersensitivity to mechanical and heat stimuli.[19] As one of the major constituents of Gram-negative bacterial cell wall, LPS is released upon cell injury and disintegration. Through binding to TLR4, LPS triggers intracellular signal cascade followed by inflammatory cytokine production, such as IL-1β, IL-6, and TNF-α, which incurs neutrophils and Mϕs recruitment into the site of inflammation as well as sensitizes the primary sensory afferents thus contributing to inflammatory pain.[22] Consistent with the process described above, LPS was used in this study and successfully presented the typical characteristics of inflammatory pain, including hyperalgesia, paw edema, neutrophil infiltration, and inflammatory responses (Fig. 1 and 2).

Increasing evidence shows that NLRP3 inflammasomes are involved in the process of inflammatory pain,[6,7] which was consistent with the enhanced expression of NF-κB (p65), NLRP3, ASC, and caspase-1 (p20) in addition to rising IL-1β levels. In view of the important role of NLPR3 inflammasomes in pain disorders, NF-κB also had been extensively studied as one of the major regulators participated in the inflammasome activation.[23] It was reported that intraplantar injection with LPS induced acute hyperalgesia in a MyD88-dependent and TRIF-independent manner in mice.[24] Our study demonstrated that the positive regulation of NF-κB transcription in NLRP3/ASC/pro-caspase-1/pro-IL-1β activation (Fig. 3). On one hand, LPS enhances NF-κB (p65) phosphorylation and then translocated into the nucleus, accelerating TNF-α and IL-6 production as well as pro-IL-1β synthesis. On the other hand, activated NF-κB switched on an initial signal that enhanced transcription of NLRP3 and pro-IL-1β, followed by a second signal that boosted the NLRP3/ASC/pro-caspase-1 inflammasomes assembly, leading to subsequent caspase-1 cleavage and further IL-1β maturation and secretion.[25]
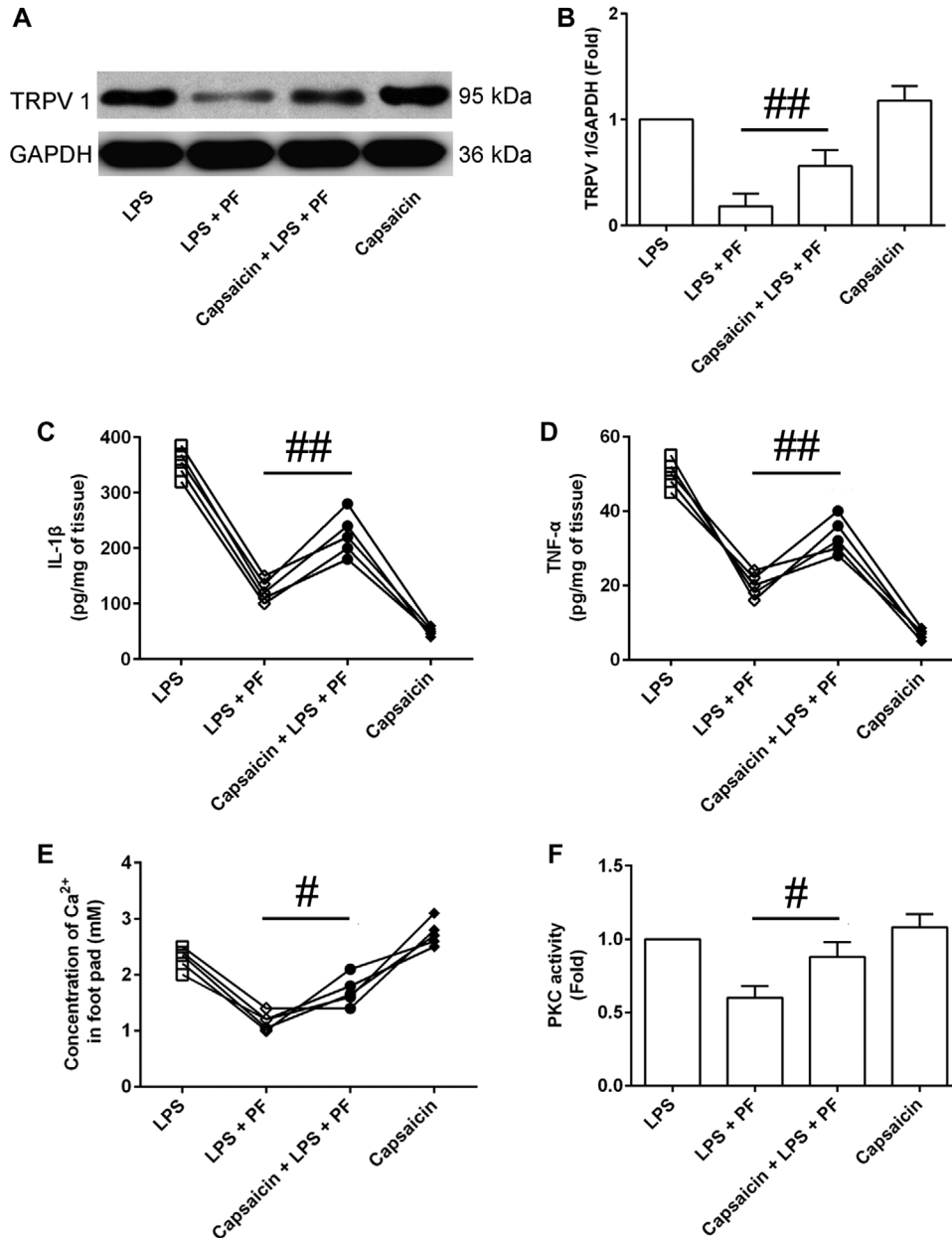
FIGURE 8 Effects of TRPV-1 agonists on cytokine production, intracellular Ca^{2+} concentration, and PKC activity. Mice was treated with capsaicin (TRPV-1 agonists) as described in the experiment II. At the end of the experiment, mice were sacrificed and samples were collected. (**A** and **B**) The expression of TRPV-1 protein in footpad tissues of different groups were measured and analyzed. A representative Western blot was displayed. (**C** and **D**) Levels of inflammatory cytokines in homogenized footpad tissues, including IL-1β and TNF-α, were measured by ELISA. (**E** and **F**) Intracellular Ca^{2+} concentration and the levels of PKC activity in different groups were detected and statistically analyzed. $^{\#}P < 0.05$ and $^{\#\#}P < 0.01$

LPS-induced increase in intracellular Ca^{2+} concentration has been found in the different cell types, such as Mϕs,[26] astrocytes,[27] and dendritic cells.[28] Some studies revealed that amplification of intracellular Ca^{2+} levels in response to LPS was due to release from endoplasmic reticulum Ca^{2+} stores.[29,30] Other publications reported that increased Ca^{2+} influx through the store-operated Ca^{2+} entry pathway was responsible for the up-regulation of cytoplasmic Ca^{2+} concentration.[31,32] Although our data indicated LPS-induced increment of intracellular Ca^{2+} levels (Fig. 5A), whether intracellular Ca^{2+} pool contributed to the changes of Ca^{2+} mobilization needs further investigation. PKCε, as a downstream molecule of Ca^{2+}-dependent signaling pathway, showed an up-regulated activity accompanying the increase of Ca^{2+} concentration during inflammatory pain (Fig. 5B). Among the PKC isoforms, PKCε was suggested to contribute to the sensitization of TRPV-1, which is a polymodal Ca^{2+}-permeable cation channel crucial to regulation of nociceptor responsiveness.[33] In PKCε-knockout mice, the hyperalgesia was reported to be decreased.[34] Simultaneously, PKCε contributed to basal and sensitizing responses of TRPV-1 to capsaicin in rat dorsal root ganglion neurons.[35] The over-expression of dominant negative PKCε was also reported to prevent
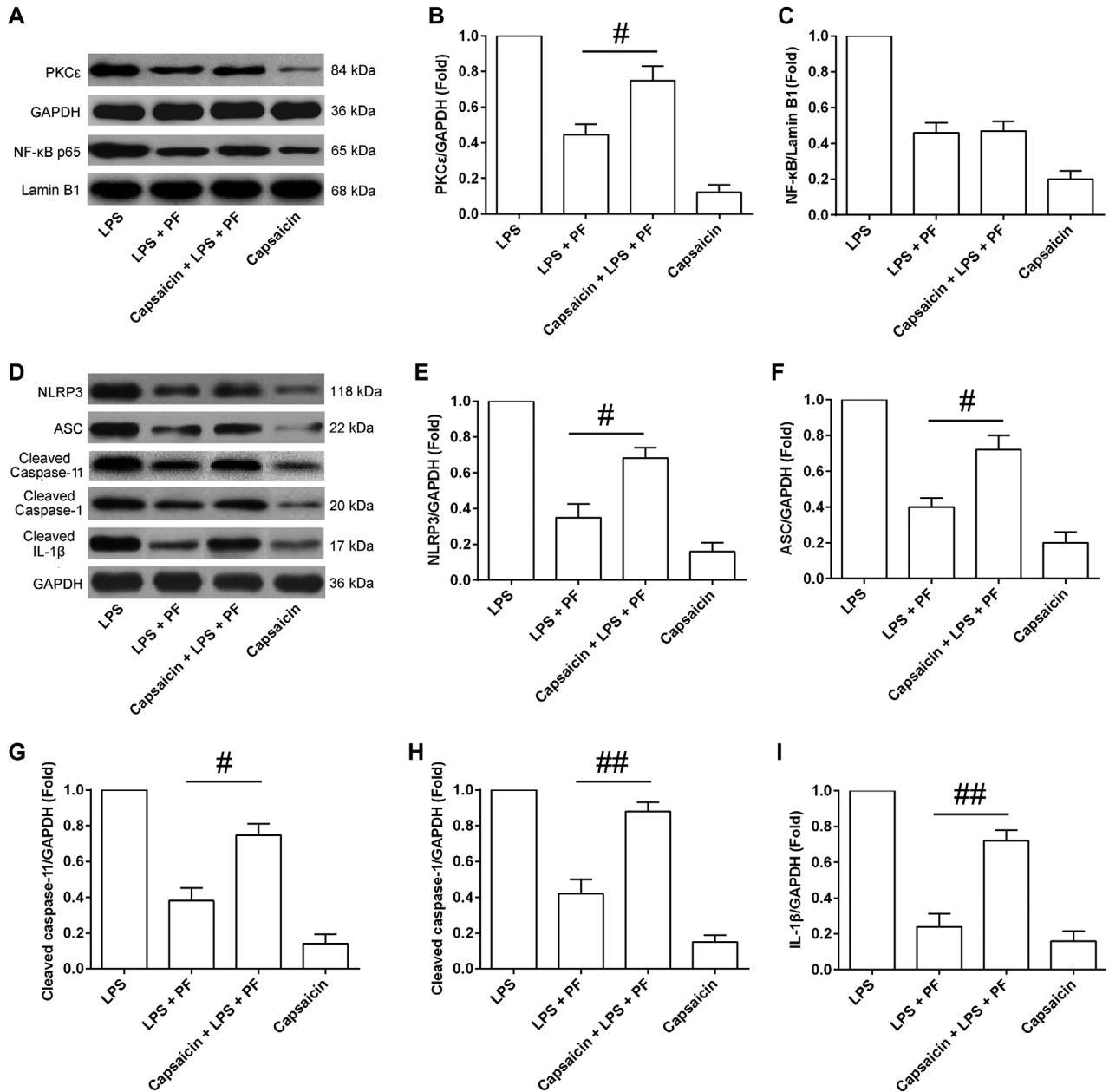
FIGURE 9 Effects of TRPV-1 agonists on NF-κB transcription and NLPR3 inflammasome activation. (**A–C**) Representative Western blot showed the expression of cytosolic PKCε and nuclear NF-κB (p65) proteins following TRPV-1 agonists treatment in inflammatory pain mice. (**D–I**) Representative Western blot indicated the expression of cytosolic NLRP3, ASC, cleaved Caspase-11 (p26), cleaved Caspase-1 (p20), and cleaved IL-1β (p17) proteins. The relative protein level (fold) was shown and statistically analyzed. GAPDH and Lamin B1 were used to confirm equal sample loading, respectively. #$P < 0.05$ and ##$P < 0.01$

TRPV-1 sensitization.[36] Considering the potential interaction between PKCε and TRPV-1, the expression of TRPV-1 was also investigated. Other PKC isoenzymes, such as PKC-α, β, δ, and ϵ, had not been completely identified in this study, further experiments would be performed in order to elucidate the details.

In recent research, the importance of TRPV-1 in regulating inflammation and pain has been highlighted. The direct activation of TRPV-1-expressing primary neurons by capsaicin induced pain and produced neurogenic inflammation.[37] During carrageenan- and CFA-

induced inflammation, the expression of TRPV-1 was up-regulated in primary nociceptive neurons and its antagonism represented an important analgesic approach to treat inflammatory pain.[38] Flavonoid reduced inflammatory pain (carrageenan-, capsaicin-, and CFA-induced mechanical and thermal hyperalgesia) by targeting TRPV-1 receptor activity,[39] suggesting the participation of TRPV-1 in the development of inflammatory hyperalgesia. TRPV-1 activity at the spinal level contributed to increased nociceptive input from primary sensory nerves to dorsal horn neurons in inflammatory pain.[40] Thus, the inhibition

of TRPV-1 activation represents an important anti-inflammatory mechanism in pain. Although the role of TRPV-1 in inflammatory hyperalgesia had been emphasized, few studies focused on the relationship between TRPV-1 and NLRP3 inflammasome activation in inflammatory pain except two publications. TRPV-1 regulated hypoxic ischemia-induced astrocyte activation and IL-1β release via inhibiting NLRP3 inflammasome activation.[41] TRPV-1 mediated cigarette smoke extract-induced damage of bronchial and alveolar epithelial cells via reduction of Ca^{2+} influx and down-regulative expression of NLRP3 and caspase-1.[42] Our results demonstrated that LPS-induced NLRP3 inflammasome activation were accompanied by increased TRPV-1 expression, a possible target of PF (Figs. 3 and 6), suggesting the possible involvement of TRPV-1-mediated NLRP3 inflammasome activation in the analgesic effect of PF in inflammatory pain.

As one of the active chemical compounds extracted from the roots of *Paeonia lactiflora*, PF has been reported to possess the analgesic activity against inflammatory pain.[12,14] It was worth noting that PF curbed NLRP3 inflammasome activation in Mϕs recruited into the inflamed skin tissues (Fig. 4), although the role of keratinocytes and T cells was not investigated. The result suggested a potential cross-correlation between TRPV-1 and PF in Mϕs. A previous study indicated activation of TLR4 on Mϕs and sensory nerves subsequently activated TRPV-1 in response to LPS stimulation.[43] TRPV-1 had been shown to protect against endotoxemia induced by LPS in mice.[44] In addition, TNF-α levels were elevated in the peritoneum, attributing to the activation of Mϕs after LPS recognition and TLR4 signaling.[45] These studies suggested the possible involvement of Mϕs in anti-inflammatory effect of PF. In this study, PF also showed the ability to relieve LPS-induced inflammatory hyperalgesia (Fig. 1–6). Furthermore, intervention of capsaicin, a specific TRPV-1 agonist, significantly abolished the analgesic effect of PF (Figs. 7 and 9D-H), which confirmed the role of TRPV-1 in anti-nociceptive characteristic of PF in inflammatory pain from the opposite side. Additionally, inhibition of NF-κB (p65) transcription under PF treatment could not be reversed in the presence of TRPV-1 agonists, suggesting that other signaling pathway or mechanisms might participate in the analgesic process of PF (Fig. 9A-C).

Based on our findings, we speculated that PF significantly curbed TRPV-1/Ca^{2+}/PKC signaling, including reduction of TRPV-1 receptors expression, intracellular Ca^{2+} levels, and downstream PKCε expression. The synergistic inhibition together, at least partly, contributed to the suppression of NF-κB transcription and led to subsequent reduction of pro-IL-1β expression. Accumulating evidence indicates that NF-κB regulates NLRP3 inflammasome in different cell types, such as epithelia, cardiomyocyte, cancer cells, and Mϕs.[46–49] In addition to the canonical NLRP3 inflammasome activation, there is another noncanonical activation that targets caspase-11, which directly induce canonical NLRP3 inflammasome activation by binding NF-κB, leading to the proteolysis and activation of pro-caspase-1 to form active caspase-1 dimers.[50,51] Additionally, activated caspase-11-dependent noncanonical inflammasome can cleave the linker loop of gasdermin D (GSDMD), resulting in cell swelling and rupture, known as pyroptosis.[52–54] PF treatment significantly suppressed the
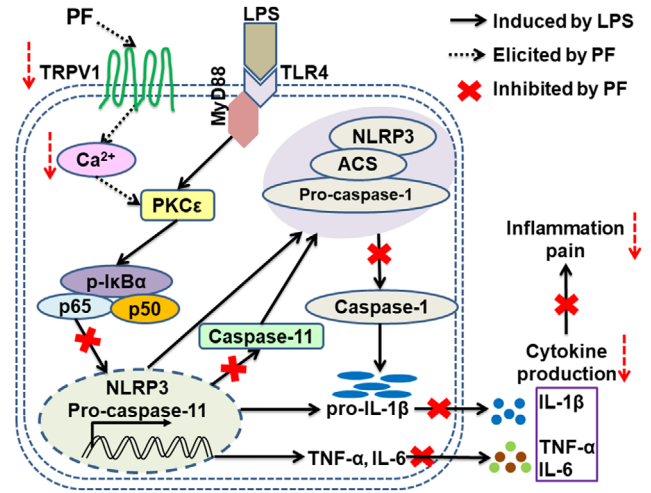
FIGURE 10 Schematic diagram of proposed mechanisms for PF on LPS-induced inflammatory pain in mice. PF treatment significantly reduced TRPV-1 expression, intracellular Ca^{2+} levels, and PKCε expression, which together contributed to the inhibition of LPS-induced NF-κB transcription, NLPR3 inflammasome activation and caspase-11-mediated non-canonical inflammasome activation, then leading to significant attenuation of cytokine production (IL-1β, TNF-α, and IL-6) in mice with inflammatory pain

expression of caspase-11 (Fig. 3), suggesting the participation of non-canonical inflammasome activation mediated by caspase-11, including canonical NLRP3 inflammasome activation as the discussion above. Upon the inhibition of NF-κB transcription and suppression of the activation of canonical NLRP3 inflammasome and caspase-11-mediated noncanonical inflammasome, thermal hyperalgesia, paw edema, and cytokine production (IL-1β, TNF-α, and IL-6) were attenuated under PF treatment in LPS-induced inflammatory pain (Fig. 10). Additional study using BAY11-7082, an inhibitor of NF-κB, would provide more evidences to clarify the details.

In summary, our results revealed the analgesic effect of PF on LPS-induced inflammatory pain in mice. The analgesic mechanism, at least partly, were related to the concomitant inhibition of NF-κB transcription and suppression of NLRP3 inflammasome activation and caspase-11-mediated noncanonical inflammasome via the regulation of TRPV-1/Ca^{2+}/PKCε mobilization. These findings suggest its potential application of PF in inflammatory pain.

AUTHORSHIP

N.Y., F.D., and Z.W. conceived and designed the study. N.Y., Q.G., and F.D. performed the experiments. N.Y. and F.D. analyzed the data. W.T. and J.C. contributed to the animal feeding and treatment. Z.W. wrote the draft manuscript. J.B. revised the final submission. Nina Yin and Qinghua Gao contributed equally to this article.

ACKNOWLEDGMENT

DISCLOSURE

The authors declare no conflict of interest.

ORCID

Zhigang Wang https://orcid.org/0000-0001-8582-0486

REFERENCES

1. Woolf CJ. What is this thing called pain?. *J Clin Invest*. 2010;120: 3742-3744.
2. Cook AD, Christensen AD, Tewari D, McMahon SB, Hamilton JA. Immune cytokines and their receptors in inflammatory pain. *Trends Immunol*. 2018;39:240-255.
3. Baral P, Udit S, Chiu IM. Pain and immunity: implications for host defence. *Nat Rev Immunol*. 2019;19:433-447.
4. Cowie AM, Dittel BN, Stucky CL. A novel sex-dependent target for the treatment of postoperative pain: the NLRP3 inflammasome. *Front Neurol*. 2019;10:622.
5. He W, Long T, Pan Q, et al. Microglial NLRP3 inflammasome activation mediates IL-1β release and contributes to central sensitization in a recurrent nitroglycerin-induced migraine model. *J Neuroinflammation*. 2019;16:78.
6. Dolunay A, Senol SP, Temiz-Resitoglu M, et al. Inhibition of NLRP3 inflammasome prevents LPS-induced inflammatory hyperalgesia in mice: contribution of NF-κB, caspase-1/11, ASC, NOX, and NOS isoforms. *Inflammation*. 2017;40:366-386.
7. Gao F, Xiang HC, Li HP, et al. Electroacupuncture inhibits NLRP3 inflammasome activation through CB2 receptors in inflammatory pain. *Brain Behav Immun*. 2018;67:91-100.
8. Morales-Lázaro SL, Simon SA, Rosenbaum T. The role of endogenous molecules in modulating pain through transient receptor potential vanilloid 1 (TRPV1). *J Physiol*. 2013;591:3109-3121.
9. Caterina MJ, Leffler A, Malmberg AB, et al. Impaired nociception and pain sensation in mice lacking the capsaicin receptor. *Science*. 2000;288:306-313.
10. Davis JB, Gray J, Gunthorpe MJ, et al. Vanilloid receptor-1 is essential for inflammatory thermal hyperalgesia. *Nature*. 2000;405:183-187.
11. Tu J, Guo Y, Hong W, et al. The regulatory effects of paeoniflorin and its derivative paeoniflorin-6'-o-benzene sulfonate CP-25 on inflammation and immune diseases. *Front Pharmacol*. 2019;10:57.
12. Tsai HY, Lin YT, Tsai CH, Chen YF. Effects of paeoniflorin on the formalin-induced nociceptive behaviour in mice. *J Ethnopharmacol*. 2001;75:267-271.
13. Zhang XJ, Li Z, Leung WM, Liu L, Xu HX, Bian ZX. The analgesic effect of paeoniflorin on neonatal maternal separation-induced visceral hyperalgesia in rats. *J Pain*. 2008;9:497-505.
14. Hu B, Xu G, Zhang X, et al. Paeoniflorin attenuates inflammatory pain by inhibiting microglial activation and Akt-NF-κB signaling in the central nervous system. *Cell Physiol Biochem*. 2018;47:842-850.
15. Huang J, Qiu L, Ding L, et al. Ginsenoside Rb1 and paeoniflorin inhibit transient receptor potential vanilloid-1-activated IL-8 and PGE_2 production in a human keratinocyte cell line HaCaT. *Int Immunopharmacol*. 2010;10:1279-1283.
16. Zucoloto AZ, Manchope MF, Staurengo-Ferrari L, et al. Probucol attenuates lipopolysaccharide-induced leukocyte recruitment and inflammatory hyperalgesia: effect on NF-κB activation and cytokine production. *Eur J Pharmacol*. 2017;809:52-63.
17. Pegorini S, Braida D, Verzoni C, et al. Capsaicin exhibits neuroprotective effects in a model of transient global cerebral ischemia in Mongolian gerbils. *Br J Pharmacol*. 2005;144:727-735.
18. Watanabe T, Kawada T, Kurosawa M, Sato A, Iwai K. Adrenal sympathetic efferent nerve and catecholamine secretion excitation caused by capsaicin in rats. *Am J Physiol*. 1988;255(1 Pt 1):E23-27.
19. Borghi SM, Carvalho TT, Staurengo-Ferrari L, et al. Vitexin inhibits inflammatory pain in mice by targeting TRPV1, oxidative stress, and cytokines. *J Nat Prod*. 2013;76:1141-1149.
20. Xue N, Wu X, Wu L, Li L, Wang F. Antinociceptive and anti-inflammatory effect of Naringenin in different nociceptive and inflammatory mice models. *Life Sci*. 2019;217:148-154.
21. Sabedra Sousa FS, Birmann PT, Bampi SR, et al. Lipopolysaccharide-induced depressive-like, anxiogenic-like and hyperalgesic behavior is attenuated by acute administration of α-(phenylselanyl) acetophenone in mice. *Neuropharmacology*. 2019;146:128-137.
22. Yoon SY, Patel D, Dougherty PM. Minocycline blocks lipopolysaccharide induced hyperalgesia by suppression of microglia but not astrocytes. *Neuroscience*. 2012;221:214-224.
23. Li Y, Liu M, Zuo Z, et al. TLR9 regulates the NF-κB-NLRP3-IL-1β pathway negatively in Salmonella-induced NKG2D-Mediated intestinal inflammation. *J Immunol*. 2017;199:761-773.
24. Calil IL, Zarpelon AC, Guerrero AT, et al. Lipopolysaccharide induces inflammatory hyperalgesia triggering a TLR4/MyD88-dependent cytokine cascade in the mice paw. *PLoS One*. 2014;9:e90013.
25. Afonina IS, Zhong Z, Karin M, Beyaert R. Limiting inflammation-the negative regulation of NF-κB and the NLRP3 inflammasome. *Nat Immunol*. 2017;18:861-869.
26. Zhou X, Yang W, Li J. Ca^{2+}- and protein kinase C-dependent signaling pathway for nuclear factor-kappaB activation, inducible nitric-oxide synthase expression, and tumor necrosis factor-alpha production in lipopolysaccharide-stimulated rat peritoneal macrophages. *J Biol Chem*. 2006;281:31337-31347.
27. Strokin M, Sergeeva M, Reiser G. Proinflammatory treatment of astrocytes with lipopolysaccharide results in augmented Ca2+ signaling through increased expression of via phospholipase A2 (iPLA2). *Am J Physiol Cell Physiol*. 2011;300:C542-549.
28. Vogel SZ, Schlickeiser S, Jürchott K, et al. TCAIM decreases T cell priming capacity of dendritic cells by inhibiting TLR-induced Ca2+ influx and IL-2 production. *J Immunol*. 2015;194:3136-3146.
29. Kandasamy K, Bezavada L, Escue RB, Parthasarathi K. Lipopolysaccharide induces endoplasmic store Ca2+-dependent inflammatory responses in lung microvessels. *PLoS One*. 2013;8:e63465.
30. Mirza KA, Tisdale MJ. Role of Ca2+ in proteolysis-inducing factor (PIF)-induced atrophy of skeletal muscle. *Cell Signal*. 2012;24: 2118-2122.
31. Velmurugan GV, Huang H, Sun H, et al. Depletion of H2S during obesity enhances store-operated Ca2+ entry in adipose tissue macrophages to increase cytokine production. *Sci Signal*. 2015;8:ra128.
32. Sun Y, Chauhan A, Sukumaran P, Sharma J, Singh BB, Mishra BB. Inhibition of store-operated calcium entry in microglia by helminth factors: implications for immune suppression in neurocysticercosis. *J Neuroinflammation*. 2014;11:210.
33. Goswami C, Kuhn J, Dina OA, et al. Estrogen destabilizes microtubules through an ion-conductivity-independent TRPV1 pathway. *J Neurochem*. 2011;117:995-1008.
34. Khasar SG, Lin YH, Martin A, et al. A novel nociceptor signaling pathway revealed in protein kinase C epsilon mutant mice. *Neuron*. 1999;24:253-260.
35. Srinivasan R, Wolfe D, Goss J, et al. Protein kinase C epsilon contributes to basal and sensitizing responses of TRPV1 to capsaicin in rat dorsal root ganglion neurons. *Eur J Neurosci*. 2008;28: 1241-1254.
36. Flynn R, Chapman K, Iftinca M, Aboushousha R, Varela D, Altier C. Targeting the transient receptor potential vanilloid type 1 (TRPV1) assembly domain attenuates inflammation-induced hypersensitivity. *J Biol Chem*. 2014;289:16675-16687.

37. Bölcskei K, Helyes Z, Szabó A, et al. Investigation of the role of TRPV1 receptors in acute and chronic nociceptive processes using gene-deficient mice. *Pain*. 2005;117:368-376.

38. Tohda C, Sasaki M, Konemura T, Sasamura T, Itoh M, Kuraishi Y. Axonal transport of VR1 capsaicin receptor mRNA in primary afferents and its participation in inflammation-induced increase in capsaicin sensitivity. *J Neurochem*. 2001;76:1628-1635.

39. Pinho-Ribeiro FA, Hohmann MS, Borghi SM, et al. Protective effects of the flavonoid hesperidin methyl chalcone in inflammation and pain in mice: role of TRPV1, oxidative stress, cytokines and NF-κB. *Chem Biol Interact*. 2015;228:88-99.

40. Huang Y, Chen SR, Chen H, Pan HL. Endogenous transient receptor potential ankyrin 1 and vanilloid 1 activity potentiates glutamatergic input to spinal lamina I neurons in inflammatory pain. *J Neurochem*. 2019;149:381-398.

41. Yang XL, Wang X, Shao L, et al. TRPV1 mediates astrocyte activation and interleukin-1β release induced by hypoxic ischemia (HI). *J Neuroinflammation*. 2019;16:114.

42. Wang M, Zhang Y, Xu M, et al. Roles of TRPA1 and TRPV1 in cigarette smoke -induced airway epithelial cell injury model. *Free Radic Biol Med*. 2019;134:229-238.

43. Meng J, Ovsepian SV, Wang J, et al. Activation of TRPV1 mediates calcitonin gene-related peptide release, which excites trigeminal sensory neurons and is attenuated by a retargeted botulinum toxin with anti-nociceptive potential. *J Neurosci*. 2009;29:4981-4992.

44. Clark N, Keeble J, Fernandes ES, et al. The transient receptor potential vanilloid 1 (TRPV1) receptor protects against the onset of sepsis after endotoxin. *FASEB J*. 2007;21:3747-3755.

45. Cunha FQ, Assreuy J, Moss DW, et al. Differential induction of nitric oxide synthase in various organs of the mouse during endotoxaemia: role of TNF-alpha and IL-1-beta. *Immunology*. 1994;81:211-215.

46. Ma M, Pei Y, Wang X, et al. LncRNA XIST mediates bovine mammary epithelial cell inflammatory response via NF-κB/NLRP3 inflammasome pathway. *Cell Prolif*. 2019;52:e12525.

47. Zou J, Yang Y, Yang Y, Liu X. Polydatin suppresses proliferation and metastasis of non-small cell lung cancer cells by inhibiting NLRP3 inflammasome activation via NF-κB pathway. *Biomed Pharmacother*. 2018;108:130-136.

48. Li X, Bian Y, Pang P, et al. Inhibition of Dectin-1 in mice ameliorates cardiac remodeling by suppressing NF-κB/NLRP3 signaling after myocardial infarction. *Int Immunopharmacol*. 2020;80:106116.

49. Martinon F, Burns K, Tschopp J. The inflammasome: a molecular platform triggering activation of inflammatory caspases and processing of proIL-beta. *Mol Cell*. 2002;10:417-426.

50. Yi YS. Regulatory roles of the caspase-11 non-canonical inflammasome in inflammatory diseases. *Immune Netw*. 2018;18:e41.

51. Yi YS. Caspase-11 non-canonical inflammasome: a critical sensor of intracellular lipopolysaccharide in macrophage-mediated inflammatory responses. *Immunology*. 2017;152:207-217.

52. Xue Y, Enosi Tuipulotu D, Tan WH, et al. Emerging activators and regulators of inflammasomes and pyroptosis. *Trends Immunol*. 2019;40:1035-1052.

53. Huang X, Feng Y, Xiong G, et al. Caspase-11, a specific sensor for intracellular lipopolysaccharide recognition, mediates the non-canonical inflammatory pathway of pyroptosis. *Cell Biosci*. 2019;9:31.

54. Zhong X, Liu M, Yao W, et al. Epigallocatechin-3-gallate attenuates microglial inflammation and neurotoxicity by suppressing the activation of canonical and noncanonical inflammasome via TLR4/NF-κB pathway. *Mol Nutr Food Res*. 2019;63:e1801230.